Available online at www.sciencedirect.com
SCIENCE DIRECT®
International Journal of Heat and Mass Transfer 49 (2006) 1384–1394
International Journal of HEAT and MASS TRANSFER
www.elsevier.com/locate/ijhmt

Study of the transient thermal wave heat transfer in a channel immersed in a bath of superfluid helium

P. Zhang [a,*], M. Murakami [b], R.Z. Wang [a]

[a] Institute of Refrigeration and Cryogenics, Shanghai Jiao Tong University, Shanghai 200030, China
[b] Graduate School of Systems and Information Engineering, University of Tsukuba, Tsukuba 305-8573, Japan

Received 3 January 2005; received in revised form 2 September 2005
Available online 29 November 2005

Abstract

Thermal wave is a very interesting phenomenon in which heat is transported in the wave mode. It is different from the ordinary Fourier heat transfer discipline in which heat is transported in the diffusive mode. In the present study, transient thermal wave (second sound wave) heat transfer in He II (superfluid helium) is numerically studied. Quantized vortices in He II, a phenomenon related to the superfluid nature, which is an important factor affecting the behavior of the thermal wave has been taken into account. The present results show that the shape of the thermal wave does not deform seriously and the amount of the heat contained in and transported by the thermal wave does not decrease as the thermal wave transmits along the channel when it is free from the quantized vortices; while the shape of the thermal wave starts to deform at the moment of the emission of the thermal wave and the amount of the heat transported by the thermal wave decreases when it is subject to the quantized vortices. The deformation is in stronger magnitude in the case of the larger heat flux. The surplus amount of the heat which cannot be carried away by the thermal wave accumulates in the thermal boundary layer formed by the dense quantized vortices and then is transferred in a diffusion-like mode. It is found that Gorter–Mellink equation is not suitable to describe the transient heat transfer process in He II.

Keywords: Thermal wave; He II; Quantized vortices; Heat transfer

1. Introduction

Thermal wave is a very interesting phenomenon in which heat is transported in the wave mode. Ordinarily, heat is considered to be transported in a diffusive way, which is generally described by the diffusive equation formulated as

$$\frac{\partial T}{\partial t} = \alpha \frac{\partial^2 T}{\partial x^2} \tag{1}$$

However, Eq. (1) is not adequate enough to describe the heat transfer process in some cases, such as, high intensity laser heating, and so on, where the thermal wave heat transfer equation should be used. A classical thermal wave equation was proposed by Cattaneo [1] and Vernotte [2], which is generally called C–V equation

$$\frac{\partial^2 T}{\partial t^2} + \frac{1}{\tau}\frac{\partial T}{\partial t} = c^2 \frac{\partial^2 T}{\partial x^2} \tag{2}$$

Essentially, Eq. (2) is hyperbolic and it supports a solution that the temperature transmits as a wave at the speed of c. One implication in Eq. (1) is the infinite heat propagation speed which is obviously questionable. Nevertheless, the relaxation time τ is very small and the diffusive equation is commonly applicable. Strictly speaking, there is still no experimental proof that supports the classical thermal wave equation.

The first experimental evidence of the thermal wave might be the successful detection of the second sound wave in superfluid helium (He II) which was carried out by Peshkov [3]. Liquid helium exists in two phases, He I and He II,

* Corresponding author. Tel.: +86 21 62933250; fax: +86 21 62932601.
E-mail address: zhangp@sjtu.edu.cn (P. Zhang).

0017-9310/$ - see front matter © 2005 Elsevier Ltd. All rights reserved.
doi:10.1016/j.ijheatmasstransfer.2005.09.031

Nomenclature

b	steepening coefficient
B_L	mutual friction coefficient
c	speed of the thermal wave
C	heat capacity
f	thermal conductance parameter or thermodynamic quantity
F_{ns}	mutual friction term
h	Planck constant
L	quantized vortex line density or length
m	mass of the helium atom
P	pressure
q	heat flux
Q	heat or energy
s	entropy
t	time
T	temperature
u	sound speed
u_{10}	first sound wave (pressure wave) at equilibrium
u_{20}	second sound wave (thermal wave) at equilibrium
v	velocity
x	distance
y	arbitrary quantity

Greek symbols

α	thermal diffusivity
γ	quantized vortices source coefficient
η	viscosity
θ	non-dimensional temperature
κ	h/m, quantum of superfluid circulation
μ	chemical energy
ρ	density
τ	relaxation time
χ_1	quantized vortices evolution coefficient
χ_2	quantized vortices decay coefficient
Φ	$x/t^{3/2}$
Ψ	$\Delta T t^{3/2}$
Δ	difference in quantity

Subscripts

b	superfluid helium bath
s	superfluid or isentropic
n	normal fluid
ns	relative value between the normal fluid and superfluid
λ	quantity at λ point
V	constant volume
P	constant pressure
L	quantized vortex line density
c	critical
h	heating

separated by a phase boundary commonly called the λ-line. Under saturated vapor pressure condition transition from He I to He II occurs at the temperature of $T_\lambda = 2.1768$ K (ITS90) which is generally called the λ-point. There is no latent heat associated with this transition as it is a kind of second order phase transition. The specific heat along the saturated vapor pressure line becomes infinite discontinuously at the λ-point. He I, a liquid phase above T_λ, is an ordinary viscous liquid; while He II, a liquid phase below T_λ, exhibits the superfluidity, which can flow through a very narrow channel in the order of μm without viscous drag.

The theory used to describe He II is Landau's two-fluid model. According to this theory, He II comprises of two components, a superfluid and a normal fluid components. The superfluid component is considered to be reduced to the ground state in energy level. The normal fluid component is in excited state and behaves like an ordinary viscous fluid. Therefore the superfluid component has zero viscosity and zero entropy, while the normal fluid component has finite viscosity and bears total entropy. They can flow through each other without any mutual interaction, and the superfluid component can flow through so narrow a slit that the normal fluid component cannot do. The superfluid and normal fluid components have their own density fields and velocity fields. The total density and the total mass flow rate are given by

$$\rho = \rho_s + \rho_n \tag{3}$$

$$\rho v = \rho_s v_s + \rho_n v_n \tag{4}$$

The ratio of the superfluid density to the total density varies from 1 to 0 as the temperature increases from below 1 K to the λ-temperature, while the ratio of the normal fluid density exhibits the contrary behavior. There are many unusual phenomena associated with He II, such as infinite thermal conductivity, fountain effect, second sound wave, and so on.

One of the most interesting characteristics of He II is the ability to transmit two kinds of sound wave: first sound wave and second sound wave. The former is a kind of ordinary pressure wave, the latter is a kind of thermal wave. The investigation of the sound propagation by small perturbation method is carried out in Refs. [4,5], and the wave speeds of the two kinds of sound wave can be written as

$$u = u_{10} = \left(\frac{\partial P}{\partial \rho}\right)_s^{1/2} \tag{5}$$

$$u = u_{20} = \left(\frac{\rho_s s^2 T}{\rho_n C_V}\right)_s^{1/2} \tag{6}$$

Two types of sound wave preserve different wave speed. The first sound wave corresponds to an ordinary pressure wave in an Euler fluid. It should be noted that in this sound

wave mode, the normal fluid and superfluid components move in phase. The propagation speed of it is about 200 m/s. On the other hand, there is no pure mass flow from macro-point of view in the thermal wave, but a relative motion between the normal fluid and superfluid components, so-called counterflow. The pressure variation associated with the thermal wave can be negligible when the amplitude of it is small enough. The thermal wave propagates at a speed of about 20 m/s, the propagation speed of the thermal wave is calculated from Eq. (6) by assuming infinitely small amplitude. A strong non-linear feature appears when the amplitude of the thermal wave is large, which cannot be regarded as isentropic anymore. In such a case, the propagation speed of the thermal wave becomes the wave amplitude ΔT dependent. The propagation speed of a point with a temperature increase ΔT in the thermal wave is described by the second order theory [5]

$$u = u_{20}\left[1 + \Delta T \frac{\partial}{\partial T} \ln\left(u_{20}^3 \frac{C_P}{T}\right)\right] = u_{20}\left[1 + b\frac{\Delta T}{T}\right] \tag{7}$$

where, u_{20} is the speed of the thermal wave for $\Delta T \to 0$, ΔT is the temperature increase within the thermal wave, b is steepening coefficient which is the temperature dependent. When the temperature T is smaller than 1.88 K, the coefficient b is positive, which indicates that points with larger wave amplitude ΔT in the thermal wave travel faster than that with smaller wave amplitude ΔT, and so the leading edge remains vertical and forms a shock, called front thermal shock wave; on the other hand, when the temperature T is larger than 1.88 K, the coefficient b is negative, a discontinuity is formed at the back of the thermal wave, then it is called back thermal shock wave. When the temperature T is slightly lower than 1.88 K, where the coefficient b is quite small, a heat pulse with larger amplitude may develop into a double thermal shock wave in which discontinuity appears both at the front and at the back of the thermal wave.

2. Two-fluid model and the quantized vortices

The hydrodynamic behavior of He II can be well described by Landau's two-fluid model. In addition to the equations for continuity, conservation of entropy and conservation of the momentum which are similar to the equations used to describe the ordinary fluids, another equation depicting the motion of the superfluid component is still needed. The two-fluid model can be formulated as

$$\begin{aligned}
&\frac{\partial \rho}{\partial t} + \nabla\cdot(\rho v) = 0\\
&\frac{\partial(\rho s)}{\partial t} + \nabla\cdot(\rho s v_n) = 0\\
&\frac{\rho_s \partial v_s}{\partial t} + \rho_s(v_s\cdot\nabla)v_s = \rho_s s\nabla T - \frac{\rho_s}{\rho}\nabla p + \frac{\rho_n\rho_s}{2\rho}\nabla v_{ns}^2\\
&\frac{\rho_n \partial v_n}{\partial t} + \rho_n(v_n\cdot\nabla)v_n = -\rho_s s\nabla T - \frac{\rho_n}{\rho}\nabla p - \frac{\rho_n\rho_s}{2\rho}\nabla v_{ns}^2 + \eta_n\nabla v_n^2
\end{aligned} \tag{8}$$

these formulas in Eq. (8) can be used to describe the isentropic process happening in He II. It is interesting to see that when He II temperature approaches λ-temperature, ρ_s approaches 0, and the fourth formula is reduced to be Navier–Stokes equation; and if He II temperature approaches absolute zero, ρ_n approaches 0, and then the third formula becomes the Euler equation. In the numerical calculation, it is more convenient to re-write Eq. (8) into another form. In the case of the one-dimensional problem, it is written as

$$\begin{aligned}
&\frac{\partial U}{\partial t} + \frac{\partial E}{\partial x} = B\\
&U = \begin{pmatrix} \rho \\ \rho s \\ v_s \\ \rho v \end{pmatrix}, \quad E = \begin{pmatrix} \rho_n v_n + \rho_s v_s \\ \rho s v_n \\ v_s^2/2 + \mu \\ p + \rho_n v_n^2 + \rho_s v_s^2 \end{pmatrix}\\
&B = \begin{pmatrix} 0 \\ F_{ns} v_{ns}/T \\ F_{ns}/\rho_s \\ \eta_n \partial v_n^2/\partial x^2 \end{pmatrix}
\end{aligned} \tag{9}$$

The vector B on the right side of Eq. (9) is zero when a hydrodynamic process occurring in He II can be regarded as isentropic. Eq. (9) can be considered as the Euler equation in the case of superfluid hydrodynamics in the ideal level. However, when the relative velocity between the normal fluid and superfluid, v_{ns}, exceeds a certain critical value, v_c, the state of He II will become superfluid turbulent [6–9], in which the hydrodynamic behavior of He II is different from that in the ideal situation. In superfluid turbulent state an additional interaction between the normal fluid and superfluid mediated by the quantized vortices will have to be taken into account. This interaction, named mutual friction, was first introduced by Gorter and Mellink [10] to help to explain the experimental heat transfer data in He II. In order to determine the macroscopic mutual friction force from the microscopic distribution of the quantized vortices, the connection between the mutual friction F_{ns} and the vortex line density (VLD) L (i.e. length of the vortex line in the unit volume) was first proposed by Vinen [11] from the experiments

$$F_{ns} = \frac{\kappa}{3}\frac{\rho_s\rho_n}{\rho} B_L L v_{ns} \tag{10}$$

where, B_L is a parameter related to the mutual friction in He II. Eq. (10) is widely accepted and adopted in the literature [6,12–14], and thus, this formula is adopted to describe the connection between the mutual friction force and the quantized vortices and it is used the numerical calculation.

In superfluid turbulent state, the isentropic process breaks down and it becomes irreversible. Consequently, the influential effect of the mutual friction on the hydrodynamic behavior of He II has to be properly dealt with. Thus, some additional items representing energy

dissipation and mutual friction are added to the right sides of the corresponding formulas in Eq. (8). And then, the non-zero items in vector B represent energy dissipation, mutual friction and the dissipation due to the viscosity of the normal fluid component, respectively. μ is the chemical energy defined as

$$d\mu = -s\,dT + \frac{1}{\rho}\,dp - \frac{1}{2}\frac{\rho_n}{\rho}\,dv_{ns}^2 \tag{11}$$

Feynman [15] firstly pointed out that the turbulent He II state is the result of the quantized vortex lines. And later, Vinen [11,16–18] proved experimentally that the vortex lines in He II are quantized and proposed a phenomenological model to describe the behavior of the quantized vortices on the base of experiments. In his model, the evolution and the decay of the vortices have both been taken into account and finally led to the following vortex line density (VLD) equation:

$$\frac{dL}{dt} = \frac{\chi_1 B_L \rho_n}{2\rho} v_{ns} L^{3/2} - \frac{\chi_2 h}{2\pi m} L^2 \tag{12}$$

where, the first term at right side is responsible for the evolution of the quantized vortices, and the second term is responsible for the decay of the quantized vortices. The parameters, χ_1 and χ_2 are describing the interaction between the normal fluid component and the quantized vortices associated with superfluid component which has to be determined experimentally. However, the above equation will lead to a problem if the initial quantized vortex line density L is zero, and the time for the quantized vortices to reach the steady value will be infinite which is obviously not correct. A source term $\gamma|v_{ns}|^{5/2}$ was added to Eq. (12) in order to correct this shortcoming, in which the coefficient γ is a strongly temperature dependent parameter. The coefficients χ_1, χ_2 and γ are temperature dependent and their values used in the calculation are cited from [11]. It should be noted here that the quantized vortices is considered to be isotropic in Vinen's VLD equation and one important assumption made in the present study is that the network of the quantized vortices generated by the propagation of the thermal wave is also isotropic.

The above Vinen's equation actually describes only the stationary condition in which the vortex line density is independent of the spatial distribution. This divergence is obvious when the hydrodynamic process cannot be regarded as stationary. Nemirovskii and Lebedev [19] modified VLD equation by adding a term of $\mathrm{div}(v_L L)$ to the left side of Eq. (12). Thus, the field property of the quantized vortices can be introduced into VLD equation and it is re-written as

$$\frac{\partial L}{\partial t} + \frac{\partial}{\partial x}(v_L L) = \frac{\chi_1 B_L \rho_n}{2\rho} v_{ns} L^{3/2} - \frac{\chi_2 h}{2\pi m} L^2 + \gamma |v_{ns}|^{5/2} \tag{13}$$

where v_L is drift velocity of the vortices tangle, which is in the order of the velocity of the superfluid component, v_s [20].

The hydrodynamics of He II can be understood by combining Landau's two-fluid model and the phenomenological description of the quantized vortices proposed by Vinen [11,16–18]. A group in Max-Planck institute investigated the thermal wave in He II both experimentally and theoretically, and the propagation of the thermal wave in convergent channel was also carried out [14,21]. Nemirovskii and Fiszdon [22] intensively reviewed the development of equations for the description of the hydrodynamic process in He II. To solve these equations, Kondaurova et al. [23] and Fiszdon and Schwerdtner [24] expanded all the hydrodynamic equations into a power series and analyzed numerically to investigate the propagation of the thermal wave in the unperturbed He II bath. In their analysis, the absence of the mass transfer was generally assumed, which directly led to $\rho v = 0$. This assumption is valid when the thermal wave is free from the quantized vortices and the amplitude of the thermal wave is small. Nevertheless, the mass transfer and the influence of the quantized vortices cannot be negligible when a large amplitude thermal wave is propagating in He II. Murakami and Iwashita [12] computed the propagation of the thermal wave in He II by using the two-fluid model and Vinen's VLD equation directly, and no more assumption was used in his analysis. However, in such an approach, the dependence of the thermodynamic quantities on v_{ns}^2 is required, which was not used in their computation. Later, Shimazaki et al. [25] conducted measurement of the thermal wave in a channel and experimentally investigated the influential effect of the quantized vortices on the thermal wave in detail.

In the present paper, the propagation of the thermal wave in a channel immersed in He II is numerically investigated. The propagation of the thermal wave both free from and subject to the quantized vortices is studied. The heat transport characteristic of the thermal wave in the interaction with the quantized vortices is also studied and the results are compared to the results obtained by using Gorter–Mellink equation as well as the experimental results in the literatures.

3. Numerical scheme

The computation model is shown in Fig. 1(a). One planar heater is placed at one end of the channel and a rectangular heat pulse with the heat flux q and the heating duration t_h is input into He II from the heater. Consequently, the thermal wave emitted in He II is a one-dimensional planar wave, which can be described by solving the one-dimensional two-fluid model, i.e. Eq. (9), with Vinen's VLD equation, i.e. Eq. (13). The boundary condition at the heater surface can be formulated as

$$\begin{aligned} &q_{input} = q, \quad 0 < t \leqslant t_h \\ &q = 0, \quad t > t_h \end{aligned} \tag{14}$$

the heat transport in He II can be written as $q = \rho s T v_n$ because the entropy is only associated with the normal fluid component. At the end of the channel, the mass transfer $\rho v = \rho_s v_s + \rho_n v_n = 0$ because of the rigid heater surface,

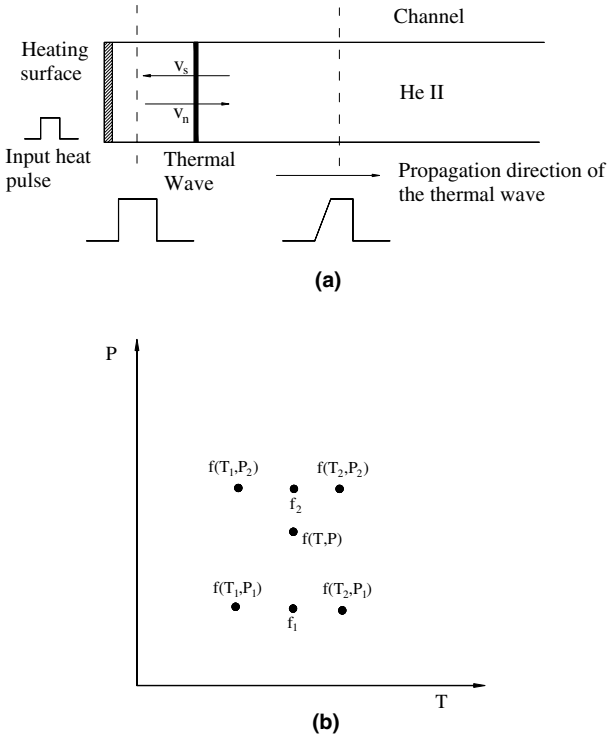

Fig. 1. (a) The schematic illustration of the computational model of the thermal wave in He II. (b) The measure for the determining of the thermodynamic quantity $f(T,P)$.

thus one has $v_{ns} = q/\rho_s sT$ as the boundary condition by combining Eqs. (3) and (4). The boundary conditions are defined in the following manner: on the basis of the fact that the thermal wave reflects on the solid boundary, they are considered as the mirror conditions, i.e. the imaginary grid points next to the boundary at both sides are symmetric. Thus, the velocity v agrees $v_{left} = -v_{right}$ at the boundary, and the thermodynamic quantities and the vortex line density agree $y_{left} = y_{right}$. The boundary condition at the other end can be treated in the same manner. However, the other end of the channel can be treated as the free boundary unless the thermal wave propagates to and reflects at the boundary.

Unlike the ordinary fluids, such as air or water, etc., the thermodynamic quantities of He II is not fully formulated but tabulated [26]. The interpolating method has to be used to determine the thermodynamic quantities. The linear interpolation is generally carried out on a P–T plane to determine a thermodynamic quantity $f(T,P)$. The interpolation is carried out by using four points, $f(T_1,P_1)$, $f(T_1,P_2)$, $f(T_2,P_1)$, $f(T_2,P_2)$, where $T_2 > T_1$, and $P_2 > P_1$. It is first carried out along T or P axis to determine f_1 and f_2. The interpolation is carried out first along T axis as an example, as can be seen in Fig. 1(b)

$$f_1 = \frac{f(T_2,P_1) - f(T_1,P_1)}{T_2 - T_1} * (T - T_1) + f(T_1,P_1) \tag{15}$$

$$f_2 = \frac{f(T_2,P_2) - f(T_1,P_2)}{T_2 - T_1} * (T - T_1) + f(T_1,P_2) \tag{16}$$

and then the interpolation is carried out along another axis

$$f(T,P) = \frac{f_2 - f_1}{P_2 - P_1} * (P - P_1) + f_1 \tag{17}$$

After the interpolation is finished, the thermodynamic quantities is corrected by the well-known relation [4]

$$\begin{aligned} \rho(P,T,v_{ns}) &= \rho(P,T) + \frac{1}{2}\rho^2 v_{ns}^2 \frac{\partial}{\partial P}\left(\frac{\rho_n}{\rho}\right) \\ s(P,T,v_{ns}) &= s(P,T) + \frac{1}{2} v_{ns}^2 \frac{\partial}{\partial T}\left(\frac{\rho_n}{\rho}\right) \\ \mu(P,T,v_{ns}) &= \mu(P,T) - \frac{1}{2}\frac{\rho_n}{\rho} v_{ns}^2 \end{aligned} \tag{18}$$

Although there are many modern numerical methods can be used to solve the Euler equations numerically, such as TVD scheme et al. These methods cannot be used since it is very difficult to obtain the Jacobian Matrix of the superfluid hydrodynamic equations, e.g. Eqs. (9) and (13). Thus, it seems more plausible to use MacCormack scheme with the flux-corrected transport (FCT). The MacCormack two-step predictor and corrector method has second order accuracy in both time and space steps. FCT is used to suppress numerical oscillation and to preserve physical discontinuity of the wave front. The standard Mac-FCT method includes eight steps, the detail of which can be found in [27].

4. Results and discussion

4.1. The thermal wave free from the quantized vortices

The propagation of the thermal wave in channel is intrinsically one-dimensional problem, although there may exist fluid–wall interaction. Turner [28] has proved such a problem is one-dimensional, and a direct proof was provided by Torczynski et al. [29] by conducting visualization experiments. Thermal wave free from the quantized vortices is investigated by using one-dimensional two-fluid model without Vinen's VLD equation in the present study. Shown in Fig. 2 is the calculation results of the propagation of the thermal wave in the channel, the time interval between the next thermal waves in the figure is 2 ms. It is seen from the figure that the amplitude of the thermal wave almost does not change as it propagates along the channel when the input heat flux is not so large, e.g. 10 W/cm^2, and its shape keeps almost the same as that of the input heat pulse when the thermal wave travels not far from the end of the channel. However, when the input heat flux is large, e.g. 30 W/cm^2, the shape of the thermal wave gradually changes and the amplitude decreases as it travels along the channel, which is due to the non-linear feature of He II thermo-fluid dynamics. Furthermore, it is seen from the figure that the shape of the thermal wave gradually changes and the rear portion of the thermal wave begins to expand and becomes longer along the channel. The traveling speed of the thermal wave depends on the temper-

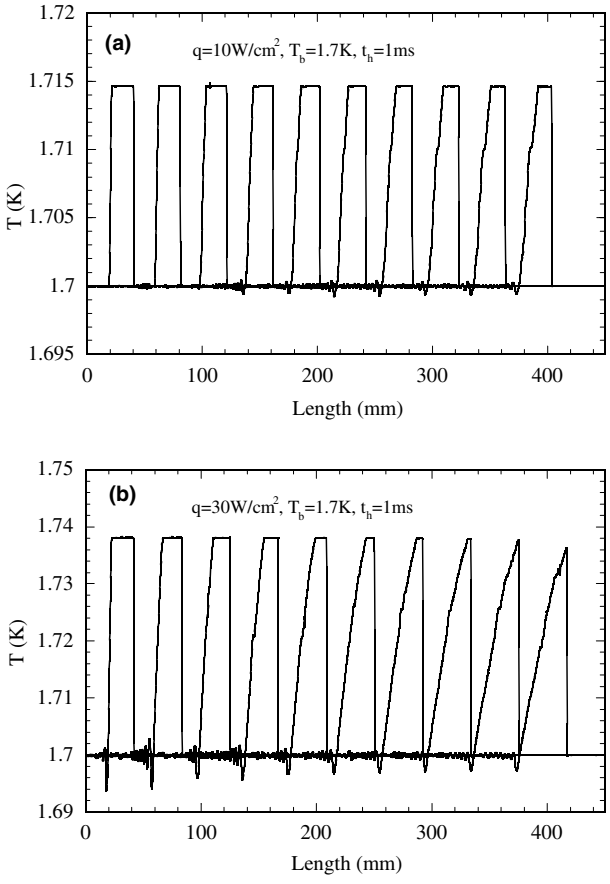

Fig. 2. The calculation results of the propagation of the thermal wave free from the quantized vortices along the channel at two heat fluxes.

ature amplitude of the thermal wave, as shown by Eq. (7). As can be seen from the thermal waves at 20 ms in Fig. 2(a) and (b), the thermal wave in Fig. 2(b) travels faster than that in Fig. 2(a) does, which is due to the point in the thermal wave with larger temperature amplitude has larger traveling speed, and it will then catch up the former point and forms a thermal shock wave. The small temperature fluctuation portions in the rear of the thermal waves are caused by the numerical oscillation.

The heat can be transported in a wave mode due to the fact of the thermal wave nature. The heat contained in and carried away by the thermal wave along the channel can be calculated as

$$Q = \int_0^L \rho(T) C_P(T) \Delta T \, dx \tag{19}$$

Shown in Fig. 3 is the ratio of the heat being carried away by the thermal wave to the total input heat. It is seen from the calculated results that almost all the input heat is carried away by the thermal wave. Although it is seen from the figure that the ratio of the heat being carried away decreases a little bit as the input heat flux increases, it is mainly attributed to the numerical error and the small dissipation effect of the FCT scheme. It can be concluded from this fact that the input heat is totally carried away by the thermal wave when it is free from the quantized vortices.

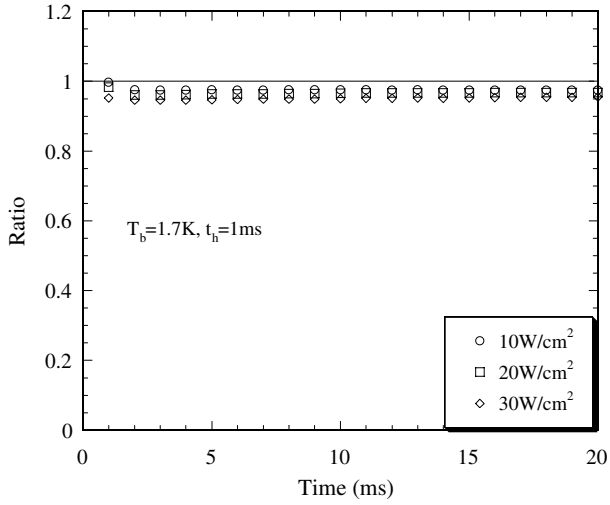

Fig. 3. The ratio of the heat contained in and carried away by the thermal wave to the total input heat when free from the quantized vortices at different heat fluxes.

4.2. The thermal wave subject to the quantized vortices

When the thermal wave is subject to the quantized vortices, there appear more complicated phenomena. The initial VLD, which can be regarded as the background of the quantized vortices, ranges generally from 1×10^4 cm^{-2} to 1×10^6 cm^{-2} [30]. Shown in Fig. 4 are the calculation results of the propagation of the thermal wave along the channel at different heat fluxes, the time interval between the next thermal waves in the figure is 2 ms. It is seen that the thermal wave differs a lot from the results in Fig. 2 as it propagates along the channel. The amplitude of the thermal wave decreases and the shape of it deforms gradually mainly due to the interaction with the quantized vortices. It is seen from Fig. 4 that the deformation of the thermal wave is generally in stronger magnitude and the amplitude of the "tail" behind the thermal wave is larger when the thermal wave does not travel far from the heater. The "tail" behind the thermal wave slowly decays and its amplitude decreases as the thermal wave propagates along the channel. The deformation of the thermal wave starts at moment of the emission of the thermal wave from the heater, which is more evident in the larger heat flux case, as can be seen in Fig. 4. The shape of the thermal wave deforms more as the heat flux increases, because the evolution of the quantized vortices is much quicker in the larger heat flux case [31] and VLD will also reach a larger steady value due to larger relative velocity v_{ns}, as shown by the first term at the right hand of Eq. (13).

The temperature histories at several fixed points are shown in Fig. 5(a). It is seen from the figure that a large temperature overshoot is following the thermal wave when the fixed point is close to the heater surface, say, 0.5 mm, which results from the thermal boundary layer caused by the mass of the quantized vortices. As the distance from the heater surface increases, this temperature overshoot

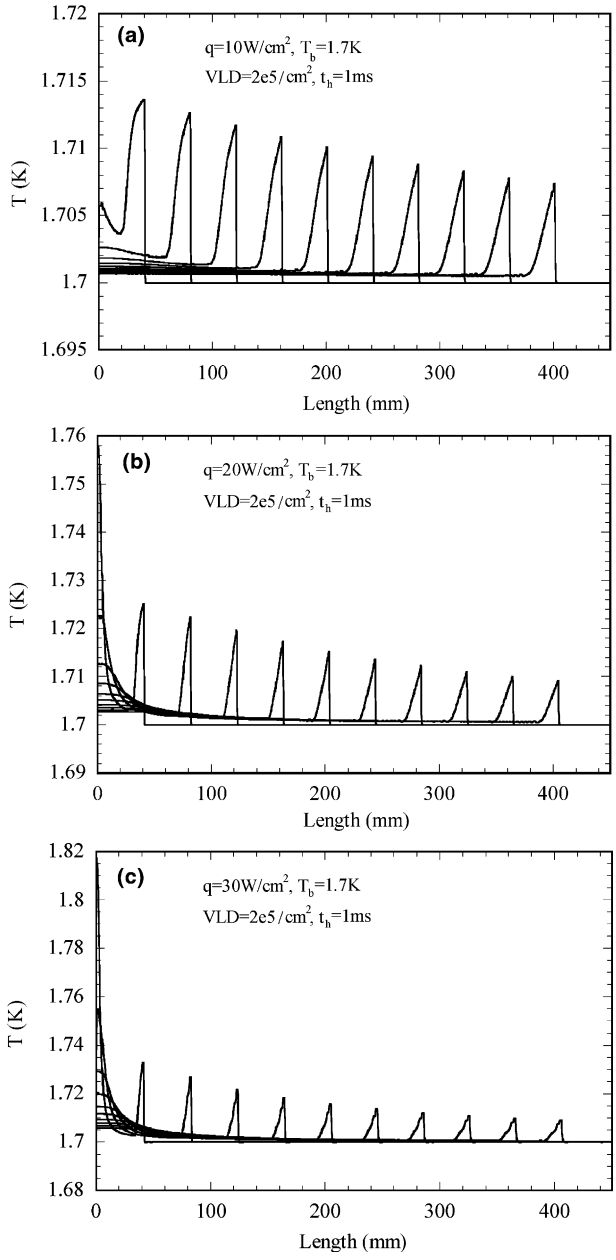

Fig. 4. The propagation of the thermal wave subject to the quantized vortices along the channel at different heat fluxes, the initial VLD = 2×10^5 cm^{-2}.

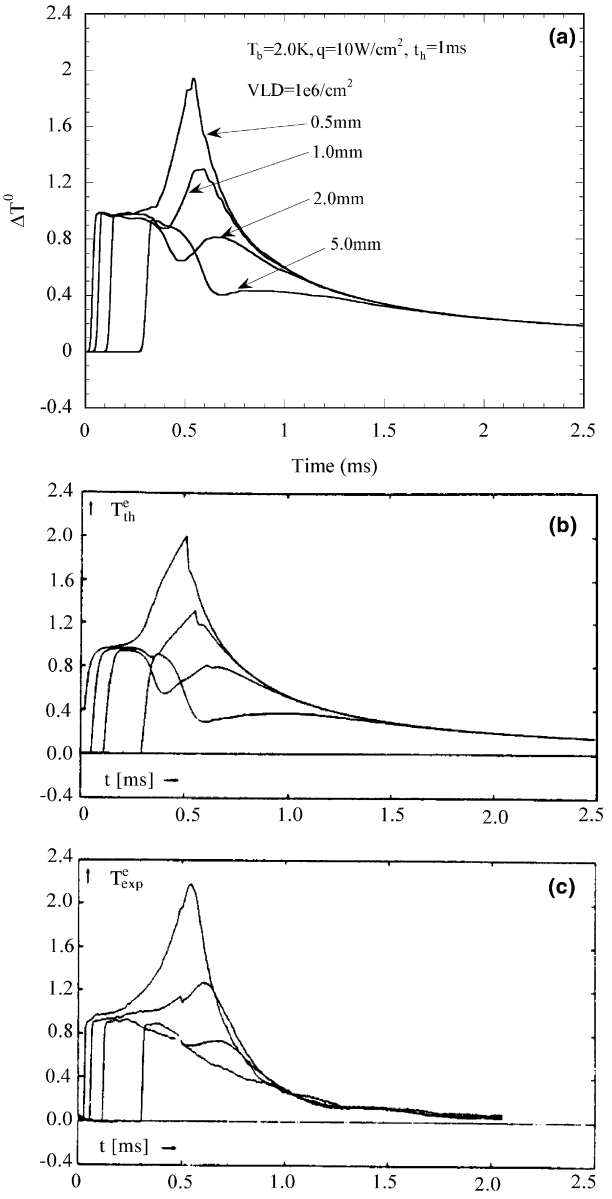

Fig. 5. The comparison of the temperature histories at different fixed distances above the heater surface to the experimental and theoretical results cited from [24]. (a) The present calculated results, (b) the calculated results cited from [24], (c) the experimental results cited from [24]. The distances are 0.5 mm, 1 mm, 2 mm and 5 mm. In Ref. [24], a parameter t_R is used to refer the repetition time of the release of the thermal wave. It is believed that when t_R is small, the background level of VLD is generally higher because the frequent release of the thermal wave in He II will cause the VLD does not have enough time to recover to the previous level, thus the next evolution of VLD will start from a relatively higher level; and vice versa, $t_R = 5$ s. The initial VLD of is 1×10^6 cm^{-2}, the same as that used in [24].

decreases quickly. In the figure, the temperature rise is normalized to $\Delta T_0 = q/\rho C_P u_{20}$, the temperature amplitude of the thermal wave at equilibrium. It is seen from Fig. 5 that the temperature increases at those points are quite quick while the temperature decreases are rather slow, which proves that the developing of the thermal boundary layer is very quick, and the decay of it is very slow and will last for a long time. Shown in Fig. 5(b) and (c) are the calculated results and the experimental ones cited from [24]. As can be seen from the figure, the present calculated results and experimental ones agree quite well with each other. The calculated results show the same time instant of the temperature overshoot as the experimental results do. As can be seen from more results shown in Fig. 6, the present calculated results agree rather well with the experimental ones and show the improvement to the calculated results in Ref. [24]. As the distance of the fixed points from the heater surface increases, the range of the temperature overshoot becomes wider and the amplitude of it also decreases.

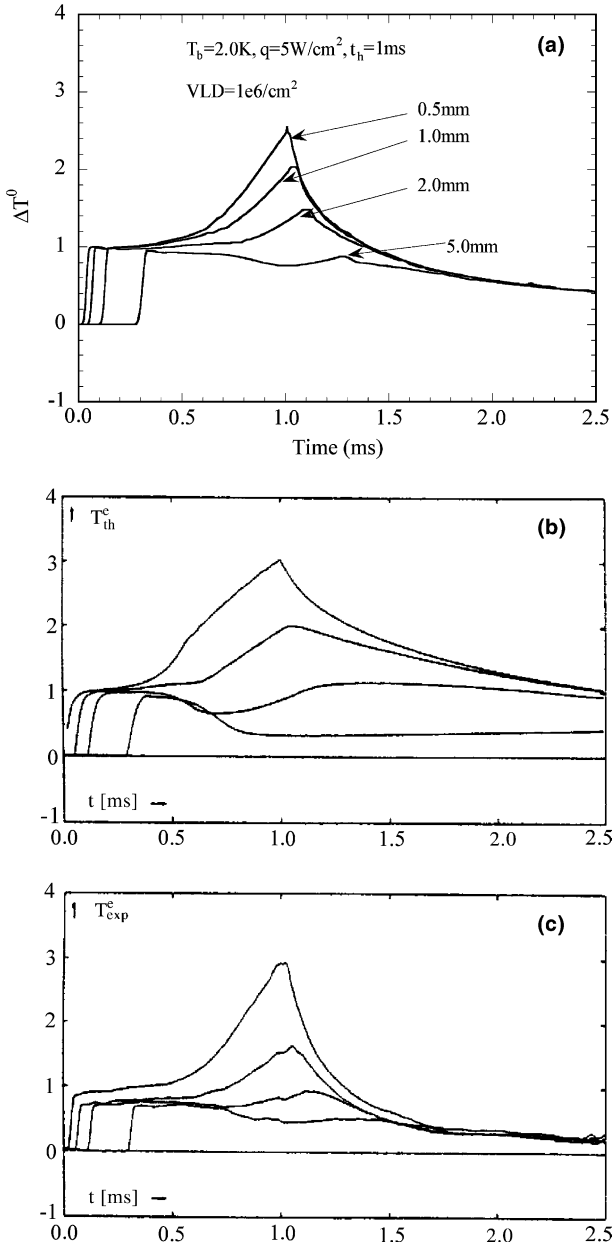

Fig. 6. The comparison of the temperature histories at different fixed distances above the heater surface to the experimental and theoretical results cited from [24]. (a) The present calculated results, (b) the calculated results cited from [24], (c) the experimental results cited from [24]. $t_R = 0.5$ s. The initial VLD $= 1 \times 10^6$ cm^{-2} is the same as that used in [24].

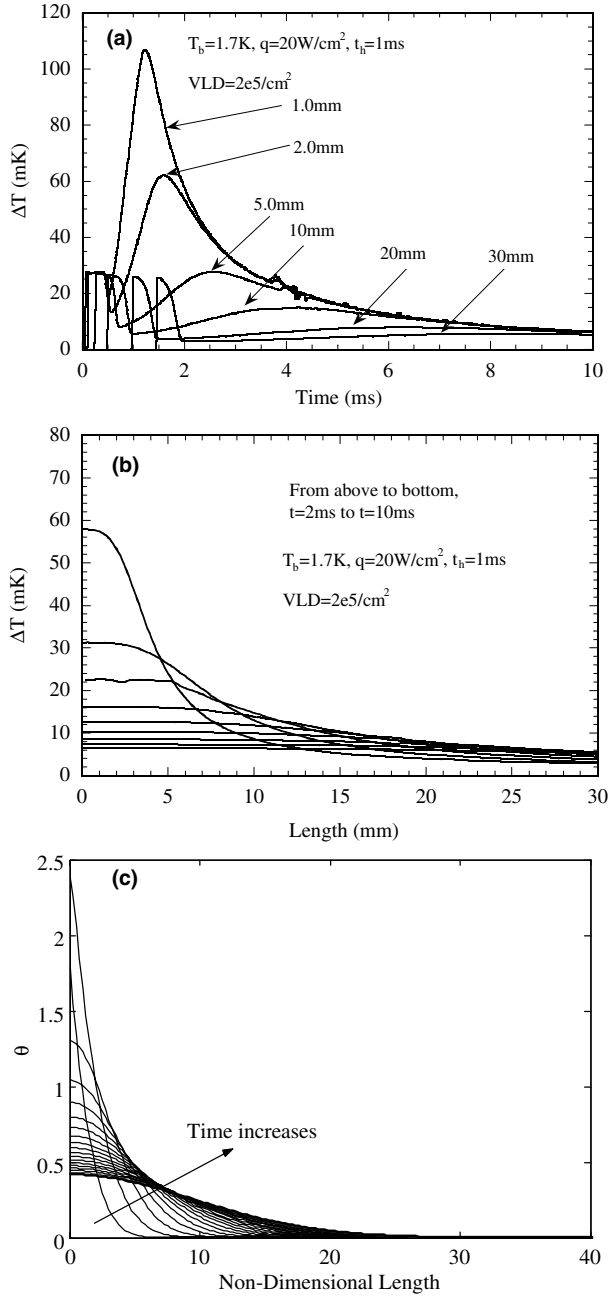

Fig. 7. (a) The computational temperature histories at different fixed distances above the heater surface, The distances are 1 mm, 2 mm, 5 mm, 10 mm, 20 mm and 30 mm, (b) the temperature distribution close to the heater surface along the channel at different time instants, (c) the temperature distribution of the diffusive heat transfer process as described by Fourier law.

The above numerical calculation is carried out in the case of the small heat flux. When the heat flux increases, the temperature overshoot for the fixed point close to the heater surface increases a lot, which can be attributed to more heat accumulated in the thermal boundary layer due to the effect of the quantized vortices, as can be seen in Fig. 7(a). It is seen from Fig. 4 that the "tail" behind the thermal wave is very long and in high temperature amplitude at larger heat flux, which is due to the slow decay of the quantized vortices tangle. Shown in Fig. 7(b) is the temperature distribution in the channel close to the heater surface. It is seen from the figure that a higher temperature region forms close to the heater surface, and the temperature of it gradually decreases. Although the heat is transported in the wave mode by the thermal wave, the superfluidity feature locally breaks down in the vicinity of the heater surface. Heat accumulates in the thermal boundary layer and is then transported in a diffusion-like mode.

Shown in Fig. 7(c) are the results of the heat transfer by Fourier heat transfer law described as

$$\frac{\partial\theta}{\partial t}=\frac{\partial^2\theta}{\partial x^2} \tag{20}$$

with the boundary condition of

$$\begin{cases} x=0, & q=-\frac{\partial\theta}{\partial x}, \\ x=L, & \theta=0 \end{cases} \quad 0<t\leqslant t_{\mathrm{h}}$$

and the initial condition of $\theta=0$. The results shown in the figure are non-dimensional. The arrow in the figure indicates the time increase. It is found from Fig. 7(b) and (c) that the decay process of the thermal boundary layer formed by the quantized vortices tangle is very similar to the diffusive heat transfer process described by Fourier law. Thus, the slow decay of this high temperature region close to the heater surface is named diffusion-like. The thermal boundary layer is remarkable in the case of the larger heat flux, while it is rather weak at smaller heat flux.

The similar method used in Section 4.1 is adopted to estimate the heat contained in and transported by the thermal wave. The thermal wave portion in this case is defined as following: the amplitude of the "tail" of the thermal wave gradually decreases in amplitude and becomes longer in spatial distribution, when the "tail" reaches the minimal value, then the end of the thermal wave is determined. It is defined in this manner because the gradual increase of temperature beyond the "tail" is caused by the quantized vortices tangle, which is essentially not the thermal wave portion. It is seen from Fig. 8 that the ratio of the heat transported by the thermal wave to the input heat gradually decreases as it propagates along the channel. This is because the quantized vortices are rapidly induced by the propagation of the thermal wave in the unperturbed He II, the counterflow between the normal fluid and superfluid components is hampered by the quantized vortices, which in turn impedes the heat transport by the thermal wave. With the evolution of the quantized vortices, a portion of the heat remains un-transported by the thermal wave and is then gradually transported in the diffusion-like process. It is further understood from the figure that the ratio of the heat transported by the thermal wave to the total input heat decreases as the heat flux increases.

When the temperature is larger, e.g. 2.1 K, the propagation of the thermal wave is shown in Fig. 9. It is seen that the shock front forms at the back of the thermal wave because the steepening coefficient is negative in this case. The interaction of the quantized vortices with the thermal wave causes the "tail" of the thermal wave becomes longer. It is interesting to see that the heat contained and transported by the thermal wave decreases a lot compared to that in the case of lower temperature, say, 1.7 K, which is due to the less efficient heat transfer capability of He II at higher temperature close to the λ-temperature.

Dresner [32] analyzed the heat transfer process by using Gorter–Mellink equation, which is similar to Fourier law in the form and is formulated as

$$\rho C_{\mathrm{P}}\frac{\partial T}{\partial t}=f\frac{\partial}{\partial x}\left(\frac{\partial T}{\partial x}\right)^{1/3} \tag{21}$$

where f is the thermal conductance parameter of He II by analogy to the thermal conductivity in Fourier law, f is in the unit of $\mathrm{W/cm^{5/3}\,K^{1/3}}$.

Essentially, Gorter–Mellink equation describes the heat transfer in He II turbulent state where the heat is considered being transported in a diffusion-like process. The analysis result of Gorter–Mellink equation is as following [32]:

$$\Phi=\frac{4/3\sqrt{3}f^{-3/2}(\rho C_{\mathrm{P}})^{-1/2}Q^2}{\left(Q^4(\rho C_{\mathrm{P}})^2f^{-6}\Psi^4+e^4\right)^{1/2}} \tag{22}$$

where $e=2.855$, Q is the total input heat, $\Psi=x/t^{3/2}$, $\Phi=\Delta T t^{3/2}$. It can be understood from the above numerical analysis that the diffusion-like heat transfer portion is following the thermal wave portion as the thermal wave is

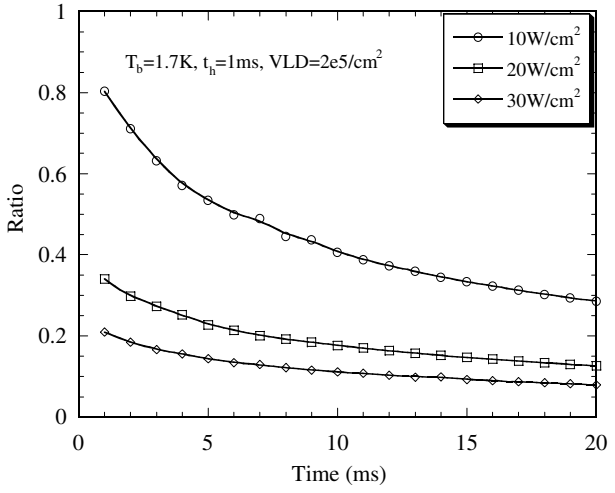

Fig. 8. The ratio of the heat contained in and carried away by the thermal wave to the total input heat when subject to the quantized vortices at different heat fluxes.

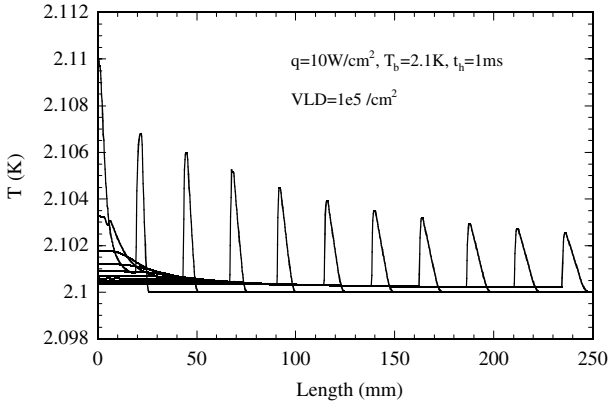

Fig. 9. The calculation results of the propagation of the thermal wave along the channel at 2.1 K.

propagating along the channel. Thus, heat is transported by both the thermal wave and the diffusion-like process. Shown in Fig. 10(a) is the comparison of the numerical and experimental results of heat transfer in He II. The solid and long-dashed lines represent the present numerical results and the symbols are the experimental results from [31] which have been re-plotted. In the figure, only the numerical results for $t = 2$ ms and $t = 8$ ms are shown for the clarity, the results of $t = 3$ ms to $t = 7$ ms lie in-between $t = 2$ ms and $t = 8$ ms. It can be understood from the figure that the numerical results and the experimental ones agree quite well with each other. It is seen from the figure that the thermal wave portion is displayed as a peak, which is essentially due to the transformation of the numerical results according to $\Psi = x/t^{3/2}$ and $\Phi = \Delta T t^{3/2}$. The experimental measurement in Ref. [31] was carried out from 2 ms to 8 ms (the moment when the heat flux is started to be released in He II is denoted as 0 ms) in the space of from the heater surface at $x = 0$ to $x = 30$ mm. Therefore, the thermal wave portion is absent in the experimental results because the propagation of the thermal wave at 2 ms has already reached around $x = 40$ mm by taking the propagation speed of the thermal wave as about 20 m/s, which is beyond the measurement range within $x = 30$ mm. The experimental results here were essentially the diffusion-like heat transfer. In Dresner's analysis, one implication is that the heat was totally transported by the diffusion-like heat transfer mode, which is generally applicable in a steady heat transfer process or long time after the heating is shut off. However, Gorter–Mellink equation is not suitable to describe the transient heat transfer process in He II because a portion of the heat is transported by the thermal wave. The dotted line in the figure is the result of Gorter–Mellink equation. The heat transfer is generally underestimated by Gorter–Mellink equation, which results in the higher temperature close to the heater surface and lower temperature far from the heater surface, as can be seen from the figure. It is worth noting here that the heat cannot be diffused by superfluid since it is inviscid. However, the mutual friction between the superfluid and normal fluid components mediated by the quantized vortices might lead to the diffusion-like heat transfer in He II. As can be understood from a recent study, the possibility of the diffusion of a packet of quantized vortices has been reported [33], which was studied by applying numerical experiments to determine the evolution of the initially localized quantized vortices, although it is not related to the heat transfer in He II directly.

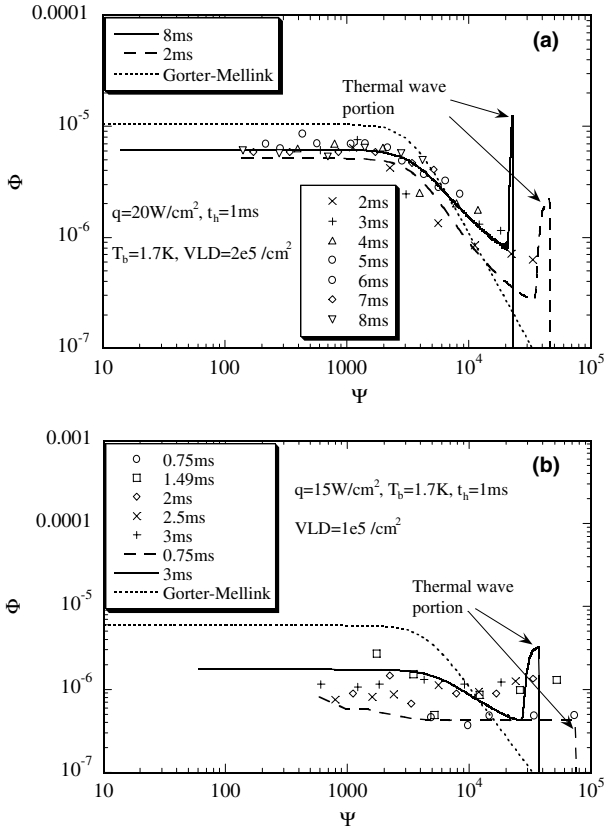

Fig. 10. The comparison of the present computational heat transfer results to the results predicted by Gorter–Mellink equation and the experimental results cited from [31]. (a) $q = 20$ W cm^2, $t_h = 1$ ms, $T_b = 1.7$ K, VLD = 2e5 cm^{-2}, (b) $q = 15$ W cm^2, $t_h = 1$ ms, $T_b = 1.7$ K, VLD = 1e5 cm^{-2}.

Shown in Fig. 10(b) is another result of the heat transfer in He II. Similar to Fig. 10(a), only the results of $t = 0.75$ ms and $t = 3$ ms are shown in the figure. As can be seen from the figure, numerical results show better agreement than Gorter–Mellink equation does. It is proven once more that Gorter–Mellink equation cannot be used in the transient heat transfer process. In such a case, numerical calculation should be carried out.

5. Conclusion

The transient thermal wave heat transfer in He II is studied numerically by using Landau's two-fluid model with Vinen's vortex line density equation. The following results are drawn from the present study:

The thermal wave almost does not deform and the input heat can be totally carried away by the thermal wave when it is free from the quantized vortices. The deformation of the thermal wave starts at the moment of the emission of the thermal wave and the wave amplitude gradually decreases as the thermal wave propagates along the channel, and the input heat cannot be totally transported by the thermal wave when it is subject to the quantized vortices. As the heat flux increases, the magnitude of the deformation of the thermal wave becomes stronger and the amount of the heat contained in and carried away by the thermal wave decreases. And as a result, the surplus amount of the heat accumulates in the thermal boundary layer formed by the dense quantized vortices close to the heater surface and results in large temperature overshoot, which is due to the counterflow is hampered by the quantized vortices. The heat contained in the thermal boundary layer is then gradually transferred in a diffusion-like way

similar to the heat transfer process described by Fourier law, which is probably the diffusion of the thermal boundary layer formed by the quantized vortices through vortex reconnection. The present numerical results show quite acceptable agreement with the experimental results and Gorter–Mellink equation generally underestimates the heat transport of He II, which results in higher temperature close to the heater surface and lower temperature far from the heater surface.

Acknowledgements

This research is jointly supported by A Foundation for the Author of National Excellent Doctoral Dissertation of PR China (200236), National Natural Science Foundation of China (50306014) and NCET.

References

[1] C. Cattaneo, A form of heat conduction equation which eliminates the paradox of instantaneous propagation, Comptes Rendus 247 (1958) 431–433.
[2] P. Vernotte, Some possible complication in the phenomena of thermal conduction, Comptes Rendus 252 (1961) 2190–2191.
[3] V. Peshkov, Second sound in helium II, J. Phys. USSR III (1944) 381–382.
[4] L.D. Landau, E.M. Lifshitz, Fluid Mechanics, Pergamon Press, Oxford, 1987, pp. 515–526.
[5] M. Khalatnikov, An Introduction to the Theory of Superfluidity, Benjamin, New York, 1965.
[6] J.T. Tough, Superfluid turbulence, in: D.F. Brewer (Ed.), Progress in Low Temperature Physics, vol. VIII, 1982, pp. 135–219.
[7] W.F. Vinen, J.J. Niemela, Quantum turbulence, J. Low Temp. Phys. 128 (2002) 167–231.
[8] C.F. Barenghi, Introduction to superfluid vortices and turbulence, in: C.F. Barenghi, R.J. Donnelly, W.F. Vinen (Eds.), Lecture Notes in Physics, vol. 571, 2001, pp. 3–14.
[9] R.J. Donnelly, C.E. Swanson, Quantum turbulence, J. Fluid Mech. 173 (1986) 387–429.
[10] C.J. Gorter, J.H. Mellink, On the irreversible processes in the liquid helium II, Physica 15 (1949) 285–304.
[11] W.F. Vinen, Mutual friction in a heat current in liquid helium II. III. Theory of the mutual friction, Proc. Roy. Soc. A 242 (1957) 493–515.
[12] M. Murakami, K. Iwashita, Numerical computation of a thermal shock wave in He II, Comput. Fluids 19 (1991) 443–451.
[13] W. Poppe, G. Stamm, J. Pakleza, Numerical and experimental studies on converging second-sound waves in a half-pipe, Physica B 176 (1992) 247–253.
[14] W.F. Fiszdon, M.v. Schwerdtner, G. Stamm, W. Popper, Temperature overshoot due to quantum turbulence during the evolution of moderate heat pulses in He II, J. Fluid Mech. 212 (1990) 663–684.
[15] R.P. Feynman, Application of quantum mechanics to liquid helium, in: C.J. Gorter (Ed.), Progress in Low Temperature Physics, vol. 1, 1955, pp. 17–53.
[16] W.F. Vinen, Mutual friction in a heat current in liquid helium II. I. Experiments on steady heat current, Proc. Roy. Soc. A 240 (1957) 114–127.
[17] W.F. Vinen, Mutual friction in a heat current in liquid helium II. II. Experiments on transient effect, Proc. Roy. Soc. A 240 (1957) 128–143.
[18] W.F. Vinen, The dictation of single quanta of circulation in liquid helium II, Proc. Roy. Soc. A 260 (1961) 218–236.
[19] S.K. Nemirovskii, V.V. Lebedev, The hydrodynamics of superfluid turbulence, Sov. Phys. JETP 57 (1983) 1009–1016.
[20] R.T. Wang, C.E. Swanson, R.J. Donnelly, Anisotropy and drift of a vortex tangle in helium II, Phys. Rev. B 36 (1987) 5240–5244.
[21] G. Stamm, Th. Olszok, M.v. Schwerdtner, D.W. Schmidt, Producing and recording converging second-sound shock waves, Cryogenics 32 (1992) 598–600.
[22] S.K. Nemirovskii, W. Fiszdon, Chaotic quantized vortices and hydrodynamic processes in Superfluid helium, Rev. Mod. Phys. 67 (1995) 37–84.
[23] L.P. Kondaurova, S.K. Nemirovskii, M.V. Nedoboiko, Mutual influence of quantum vortices and heat pulses in superfluid helium, Low Temp. Phys. 25 (1999) 475–481.
[24] W. Fiszdon, M.v. Schwerdtner, Influence of quantum turbulence on the evolution of moderate plane second sound heat pulses in helium II, J. Low Temp. Phys. 75 (1989) 253–267.
[25] T. Shimazaki, M. Murakami, T. Iida, Second sound wave heat transfer, thermal boundary layer formation and boiling: highly transient heat transport phenomena in He II, Cryogenics 35 (1995) 645–651.
[26] CRYODATA. HEPAK software, 1993.
[27] C.A.J. Fletcher, Computational Techniques for Fluid Dynamics. VII. Specific Techniques for Different Flow Categories, Springer-Verlag, 1988.
[28] T.N. Turner, Using second-sound shock waves to probe the intrinsic critical velocity of liquid helium II, Phys. Fluids 26 (1983) 3227–3241.
[29] J.R. Torczynski, D. Gerthsen, Th. Roesgen, Flow visualization of shock waves in liquid helium II, Proc. LT-17, 1984, pp. 67–68.
[30] Y.A. Sergeev, C.F. Barenghi, Interaction of weakly nonlinear second sound waves with a vortex tangle in helium II, J. Low Temp. Phys. 127 (2002) 203–214.
[31] T. Shimazaki, Experimental study of highly transient thermo-fluid dynamic phenomena in He II, PhD dissertation, University of Tsukuba, 1996.
[32] L. Dresner, Transient heat transfer in superfluid helium—Part II, Adv. Cryo. Eng. 29 (1984) 323–333.
[33] C.F. Barenghi, D.C. Samuels, Evaporation of a packet of quantized vorticity, Phys. Rev. Lett. 89 (2002) 155302.